JTE HCM-UTE
ISSN: 2615-9740

JOURNAL OF TECHNICAL EDUCATION SCIENCE
Ho Chi Minh City University of Technology and Engineering
Website: https://jte.edu.vn
Email: jte@hcmute.edu.vn

A Study on the Calculation, Design, and Fabrication of a Radio Frequency Drying System

Lieu Le Quang[1], Liviu Giurgiulescu[2], Hung Do Xuan[3], Dzung Nguyen Tan[4*]
[1]*College of Fishery and Food Technology, Hai Phong City, Vietnam*
[2]*Technical University of Cluj Napoca, North Universitary Center of Baia Mare, Romania*
[3]*National College of Education, Ho Chi Minh City, Vietnam*
[4]*Ho Chi Minh City University of Technology and Engineering, Vietnam*

[*]Corresponding author. *Email: tandzung072@hcmute.edu.vn*.

ARTICLE INFO

Received: 23/02/2026
Revised: 06/03/2026
Accepted: 23/03/2026
Published online: 24/03/2026

KEYWORDS

Radio Frequency Drying;
High-Frequency Electric Field Drying;
Dielectric Drying Using Radio Frequency Energy;
Radio Frequency-Assisted Drying;
Industrial-Scale Radio Frequency Dryer.

ABSTRACT

This study presents the results of the calculation, design, and fabrication of a high-frequency electric field (radio frequency, RF) drying system with a capacity of 1000 kg per batch and a drying time of 1.2 hours per batch. Based on material and energy balance analyses, the principal technical parameters of the system were determined, providing the foundation for mechanical design, installation of the RF power supply, and development of the automatic control system. After completion, the system was experimentally operated to evaluate its operational stability and performance efficiency through the drying of seasoned anchovies, in comparison with a conventional hot-air convective drying method. The experimental results show that the system operated stably throughout the entire drying process, with a rapid moisture reduction rate and a drying time reduced by approximately 90% compared with conventional convective drying. The specific energy consumption was 10–12% lower, while the sensory quality of the product was higher (9.4 compared with 8.6) across the entire investigated moisture range, with an optimal moisture content of approximately 8–9%. These findings confirm the high feasibility of the radio frequency (RF) drying system, demonstrating that it meets technological requirements and has strong potential for application in industrial-scale production.

Doi: https://doi.org/10.54644/jte.2026.2106

1. Introduction

Drying is one of the fundamental and decisive operations in post-harvest technology and in the processing of foods, agricultural products, medicinal materials, as well as various other biological materials [1]-[4]. The primary objective of the drying process is to reduce the moisture content of materials to a safe storage level, thereby inhibiting microbial and enzymatic activities while preserving, to the greatest extent possible, the sensory attributes and nutritional value of the product. Conventional drying methods such as hot-air convective drying, rotary drum drying, fluidized-bed drying, and infrared radiation drying are mainly based on external heat transfer from the surrounding medium to the material surface. Subsequently, heat is conducted inward, accompanied by moisture diffusion from the interior to the surface [1]-[6]. This mechanism often results in significant temperature and moisture gradients between the surface and the core of the material, leading to surface overheating, structural cracking, color deterioration, nutrient losses, and high energy consumption due to prolonged drying times [6]. In the context of increasing demands for improved energy efficiency, shortened processing time, and enhanced product quality, volumetric heating technologies based on high-frequency electric fields have attracted growing research interest and wider industrial application [1], [6].

Radio frequency drying (RF drying) is a technique that employs electromagnetic fields at frequencies lower than those of microwaves (typically within the range of 1–300 MHz, with common industrial frequencies of 13.56 MHz, 27.12 MHz, and 40.68 MHz) to heat dielectric materials [1], [6], [7]. Under the action of an alternating electric field established between two electrodes, polar molecules—particularly water molecules—continuously oscillate in response to the changing field direction,

resulting in dielectric loss and direct heat generation throughout the entire volume of the material [7]. In contrast to the surface heating mechanism of convective drying, radio frequency heating is a volumetric heating process, in which heat is generated simultaneously within the interior of the material. This significantly shortens the heating-up period and accelerates moisture evaporation. Owing to its longer wavelength compared to microwaves, radio frequency energy provides deeper penetration, reduces localized hot spots, and is particularly suitable for large-sized materials, thick layers, or products with high moisture content. Consequently, this technology has been applied in engineered wood drying, bulk agricultural product drying, grain disinfestation, seafood drying, and the processing of various high-value food products [2]-[3], [8].

Worldwide, research on radio frequency (RF) drying has focused primarily on three main directions: (i) determination and modeling of the dielectric properties of materials (dielectric constant and dielectric loss factor) as functions of moisture content, temperature, and frequency; (ii) development of coupled heat and mass transfer models integrated with electromagnetic field analysis to predict temperature and moisture distributions during the drying process; and (iii) optimization of equipment configurations, including electrode spacing, drying chamber geometry, power supply modes, and hybridization with auxiliary drying methods such as hot-air convection or vacuum drying. However, due to the nonlinear behavior of moist materials and the strong dependence of dielectric loss on moisture content, RF drying inherently carries the risk of non-uniform electric field distribution, electrical discharge (arcing), or localized overheating if the system is not properly designed and controlled [6]-[7]. Therefore, accurate calculation of the required RF power, power density distribution within the material, and overall system energy balance constitutes the core aspects of equipment design.

In Vietnam, although the demand for advanced drying technologies for agricultural and food products has been steadily increasing, most radio frequency equipment is still imported at high cost and remains limited in terms of localized design and manufacturing. Domestic studies have primarily been conducted at laboratory scale or have focused on evaluating the effects of drying conditions on product quality, whereas research on systematic calculation, design, fabrication, and integration of complete RF drying systems remains limited [6]-[9]. Therefore, the study of calculation, design, and fabrication of a radio frequency drying system based on the integration of heat and mass transfer theory with dielectric theory and high-frequency engineering is of significant scientific and practical importance [8], [9]. This research not only contributes to technological mastery, energy efficiency optimization, and improvement of dried product quality, but also establishes a foundation for the development, localization, and commercialization of radio frequency drying equipment tailored to domestic production conditions, thereby meeting the modernization demands of the food and agricultural processing industries.

2. Materials and Methods

2.1. Materials

The drying material is seasoned anchovies. The initial moisture content of the raw material prior to drying is $W_1 = 70\%$, and the final moisture content required for the product is $W_2 = 8\%$. The bulk density of the seasoned anchovies is approximately $\rho \approx 550$ kg/m^3, [9], [10]. In the figure, the label needs to be corrected

2.2. Design Calculation Method

2.2.1. Design Input Data

- Equipment capacity: $G_1 = 1000$ kg/batch; drying time per batch $\tau_s = 1.2$h;
- Initial temperature of the raw material: $t'_1 = 25^0$C; final product temperature: $t'_2 = 65^0$C
- Average specific heat capacity of dry matter in seasoned anchovies: $C_{ck} = 1.3$ kJ/(kg.K);
- Specific heat capacity of water: $C_n = 4.186$ kJ/(kg.K);
- Latent heat of vaporization of water at 65^0C: $L_v = 2350$ kJ/kg;
- Assumed overall heat transfer coefficient through the drying chamber wall: $K = 1.39$ W/(m^2.K);

2.2.2. Mass Balance Calculation

- Final product mass after drying:

$$G_2 = G_1 \frac{100 - W_1}{100 - W_2}, \text{ kg/batch} \quad (1)$$

- Mass of water evaporated during drying:

$$W = G_1 - G_2, \text{ kg/batch} \quad (2)$$

- Mass of dry matter in the raw material:

$$G_{ck} = G_1(1 - W_1), \text{ kg/batch} \quad (3)$$

- Mass of moisture in the raw material:

$$W_n = G_1.W_1, \text{ kg/batch} \quad (4)$$

- Mass of residual moisture in the dried product:

$$W_{cl} = W_n - W, \text{ kg/batch} \quad (5)$$

2.2.3. Energy balance calculation

Based on the principle of energy conservation, the heat loss Q (kW) in the drying process is equal to the thermal energy supplied by the high-frequency generator. Hence, the energy balance equation is expressed as follows [11], [12]:

$$Q = \frac{Q_1 + Q_2 + Q_3 + Q_4 + Q_5}{3600 \times \tau_s} + Q_6 = \frac{\sum Q}{3600 \times \tau_s} + Q_6, \text{ kW} \quad (6)$$

where:

Q_1 (kJ/batch) – Thermal energy required to heat the dry solids of the seasoned anchovies from $t'_1 = 25^0C$ to $t'_2 = 65^0C$;

Q_2 (kJ/batch) - Thermal energy required to heat the moisture present in the seasoned anchovies from $t'_1 = 25^0C$ to $t'_2 = 65^0C$;

Q_3 (kJ/batch) - Thermal energy required for the evaporation of W (kg per batch) of moisture in the seasoned anchovies;

Q_4 (kJ/batch) - Thermal energy required to heat the trays holding the seasoned anchovies from $t'_1 = 25^0C$ to $t'_2 = 65^0C$;

Q_5 (kJ/batch) - Thermal energy required to heat the air inside the drying chamber from $t_1 = 25^0C$ to $t_2 = 65^0C$;

Q_6 (kW) – Thermal losses through the enclosure of the high-frequency drying chamber;

a. Calculation of Q_1

Q_1 (kJ/batch) – The thermal energy required to heat the dry solids of the seasoned anchovies from $t'_1 = 25^0C$ to $t'_2 = 65^0C$ is calculated using the following equation:

$$Q_1 = C_{ck} \times G_{ck} \times (t'_2 - t'_1), \text{ kJ/batch} \quad (7)$$

b. Calculation of Q_2

Q_2 (kJ/batch) - Thermal energy required to heat the moisture present in the seasoned anchovies from $t'_1 = 25^0C$ to $t'_2 = 65^0C$ is calculated using the following equation:

$$Q_2 = C_{pn} \times W_n \times (t'_2 - t'_1), \text{ kJ/batch} \quad (8)$$

c. Calculation of Q_3

Q_3 (kJ/batch) - Thermal energy required for the evaporation of W (kg per batch) of moisture in the seasoned anchovies is calculated using the following equation:

$$Q_3 = W \times L_v, \text{ kJ/batch} \quad (9)$$

d. Calculation of Q_4

Q_4 (kJ/batch) - The thermal energy required to heat the trays holding the seasoned anchovies from $t'_1 = 25^0$C to $t'_2 = 65^0$C is calculated using the following equation:

$$Q_4 = C_{pinox} \times G_k \times (t'_2 - t'_1), \text{ kJ/batch} \quad (10)$$

where: the specific heat capacity of stainless steel 304 is $C_{pinox} = 0.48$ kJ/(kg.K); G_k (kg) is the mass of the trays containing the seasoned anchovies.

e. Calculation of Q_5

Q_5 (kJ/batch) - Thermal energy required to heat the air inside the drying chamber from $t_1 = 25^0$C to $t_2 = 65^0$C is calculated using the following equation:

$$Q_5 = C_{pk} \times G_{kk} \times (t'_2 - t'_1), \text{ kJ/batch} \quad (11)$$

where: the average specific heat capacity of air is $C_{pk} = 1.006$ kJ/(kg.K);

f. Calculation of Q_6

Q_6 (kW) – Thermal losses through the enclosure of the high-frequency drying chamber is calculated using the following equation:

$$Q_6 = K \times F_t \times (t_{f2} - t_{f1}).10^{-3}, \text{ kW} \quad (12)$$

2.2.4. Calculation of the volume of the raw material

The average bulk density of the seasoned anchovies is $\rho \approx 550$ kg/m^3. Accordingly, the volume of the raw material (V_{ngl}) is calculated using the following expression [13]:

$$V_{ngl} = \frac{G}{\rho}, \text{ m}^3 \quad (13)$$

2.2.5. Selection of the operating frequency f, determination of the electrode gap d, and calculation of the electric field intensity E and applied voltage U

- Dielectric power absorbed by the material:

$$P = 2\pi f \times \varepsilon_0 \times \varepsilon'' \times E^2 \times V, \text{ W} \quad (14)$$

Where:

- P - dielectric power absorbed by the material (W);
- f - frequency (Hz), f = 27 MHz = 2.7×10^7 Hz;
- $\varepsilon_0 = 8.854\times10^{-12}$ F/m - permittivity of free space (vacuum permittivity);
- ε'' - dielectric loss factor of the material, $\varepsilon'' = (8 \div 15) = 8$;
- E - electric field intensity (V/m);
- V - volume of the material exposed to the electric field (m³);

Therefore,
$$E = \sqrt{\frac{P}{2\pi f \times \varepsilon_0 \times \varepsilon'' \times V}}, \text{ V/m} \quad (15)$$

- Applied voltage across the drying electrodes:

$$U = E \times d \text{ và } U_{lv} = k_{lv} \times U \quad (16)$$

Where: d = (50 ÷ 120) mm = 100 mm = 0.1 m is distance between the two electrodes;

k_{lv} = (1.1 ÷ 1.5) = 1.5 is safety coefficient for the applied drying voltage;

2.2.6. Calculation of the drying chamber dimensions

The high-frequency drying chamber is designed as a rectangular box with dimensions D×R×H (m×m×m). The chamber consists of multiple compartments, and in each compartment, two electrodes (upper and lower electrodes) are installed at the top and bottom, respectively. Therefore, the height of each compartment is equal to the distance between the two electrodes, i.e., h = d (m). The lower electrode of each compartment must withstand the load of the tray containing the drying material [8], [9].

- Electromagnetic penetration depth into the moist material during drying:

$$d_e = \frac{c}{2\pi f \sqrt{2\varepsilon''}}, \text{ m} \quad (17)$$

Where: d_e (m) - penetration depth;

$c = 3 \times 10^8$ m/s – speed of light in vacuum;

$f = 27$ MHz $= 2.7 \times 10^7$ Hz – frequency of the high-frequency current;

$\varepsilon'' = 8$ – dielectric loss factor of the materia.

- Determination of the drying layer thickness of seasoned anchovy material:

In order to reach the target moisture content within 1.2 hours, the seasoned anchovy layer should be uniformly spread in a thin layer. A smaller thickness improves electromagnetic field penetration, ensuring more effective volumetric heating and moisture diffusion during the drying process.

On this basis, the thickness of the seasoned anchovy drying layer is calculated and selected within the range of:

$$d_{vl} = (0.05 \div 0.1) \times d_e \quad (18)$$

- Total required tray area for holding seasoned anchovies:

$$A_{sum} = \frac{V_{ngl}}{d_{vl}}, \text{ m}^2 \quad (19)$$

- Determination of the electrode plate area for each drying level:

The electrode plate area for each level is designed to be equal to the internal cross-sectional area of the drying chamber. This area also corresponds to the tray-supporting surface for seasoned anchovies in each drying compartment. The drying chamber area is calculated according to the following expression: [8]-[10]:

$$A_{chamber} = D \times R, \text{ m}^2 \quad (20)$$

The selected value is: D = 3.2 m; R = 2.4 m;

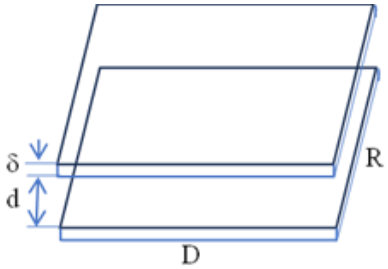

Figure 1. *Arrangement of two parallel drying electrodes.*

- Calculation of the number of drying trays (levels) in the drying chamber:

The number of drying levels (or racks), corresponding to the number of electrode pairs installed in the high-frequency drying chamber, is determined according to the following expression:

$$N = \frac{A_{sum}}{A_{chamber}} \quad (21)$$

- Calculation of the drying chamber height:

The drying chamber was designed with 10 tiers. Each tier is equipped with two electrodes (upper and lower), separated by a distance of d = 0.1m. The total thickness of the drying tray and the electrode assembly at each tier is δ = 40mm = 0.04m (see Figure 1). Accordingly, the height of the drying chamber is determined using the following equation [11], [12]:

$$H = N \times d + 2 \times N \times \delta, \text{ m} \quad (22)$$

2.2.7. Calculation of the exhaust and supply fan power for the drying chamber

- Calculation of the drying chamber volume:

$$L_q = n \times V_{chamber}, \text{ m}^3 \quad (23)$$

- Calculation of the exhaust and supply fan flow rate:

$$V_{chamber} = D \times R \times H, \text{ m}^3 \quad (24)$$

Where: n is the number of air changes within the drying chamber during one drying batch.

- Electric motor power of the exhaust fan:

$$N_{mq} = k_q \times \frac{\Delta P_q \times Q}{1000 \eta_H \eta_V \eta_{ck}}, \text{ kW} \quad (25)$$

Where: k_q = 1.10 ÷ 1.15 is the safety load factor; select k_q = 1.15;

η_H = 0.95 ÷ 1.00 is the hydraulic efficiency; select η_H = 0.95;

η_V = 0.95 ÷ 1.00 is the volumetric efficiency; select η_V = 0.95;

η_{ck} = 0.90 ÷ 1.00 is the mechanical transmission efficiency of the electric motor; select η_{ck} = 0.9;

ΔP_q = (0.1 ÷ 0.5)at is the total pressure loss of the drying medium along the entire flow path;

2.3. Determination of the technological parameters of the drying process

- Determination of the drying air temperature T (^{0}C) using a temperature sensor integrated into the measurement and control system of the drying process [13].

- To determine the drying time t (min), the system employed a computer-based timer preprogrammed in the control software, ensuring high accuracy, [13].

2.4. Determination of the objective functions of the drying process

2.4.1. Determination of the moisture content of the drying material

The moisture content of the seasoned anchovy product dried using high-frequency electric field drying is determined as follows, [11], [12]:

$$y_1 = W_e(\%) = 100 - \frac{G_1}{G_e} \times (100 - W_1), \% \quad (26)$$

Where: G_1 (g) – mass of the drying material sample; G_e (g) – mass of the seasoned anchovy product after drying; W_1 (%) – initial moisture content of the drying material; W_e (%) – moisture content of the product after drying.

2.4.2. Determination of energy consumption

A wattmeter was used to determine the specific energy consumption per kilogram of product. The energy required for the high-frequency electric field drying process to produce 1 kg of finished product is calculated using the following equation [12], [13]:

$$y_2 = \frac{P \times \tau_s}{G} = \frac{U \times I \times \cos\varphi}{G} \times \tau_s, \text{ kWh/kg} \quad (27)$$

In which: y_1 (kWh/kg) is the specific energy consumption per 1 kg of product; G (kg) is the mass of the product; U (V), I (A), and cosφ are the voltage, current, and power factor of the power supply for the drying system, respectively, as measured by the integrated wattmeter; τ_s is drying time.

2.4.3. Determination of the sensory quality attributes of the product

$$y_3 = \text{Sensory evaluation scores assigned by expert panelists} \quad (28)$$

3. Results and discussion

3.1. Schematic diagram of the drying system to be designed and calculated

To calculate, design, and fabricate a high-frequency electric field drying system, it is essential to first develop an appropriate schematic diagram. A well-established and technically sound schematic serves as the fundamental basis for accurate design calculations. Only with a correct conceptual design can the fabricated drying system be effectively implemented in practical production. The results of this study are presented in Figure 2.

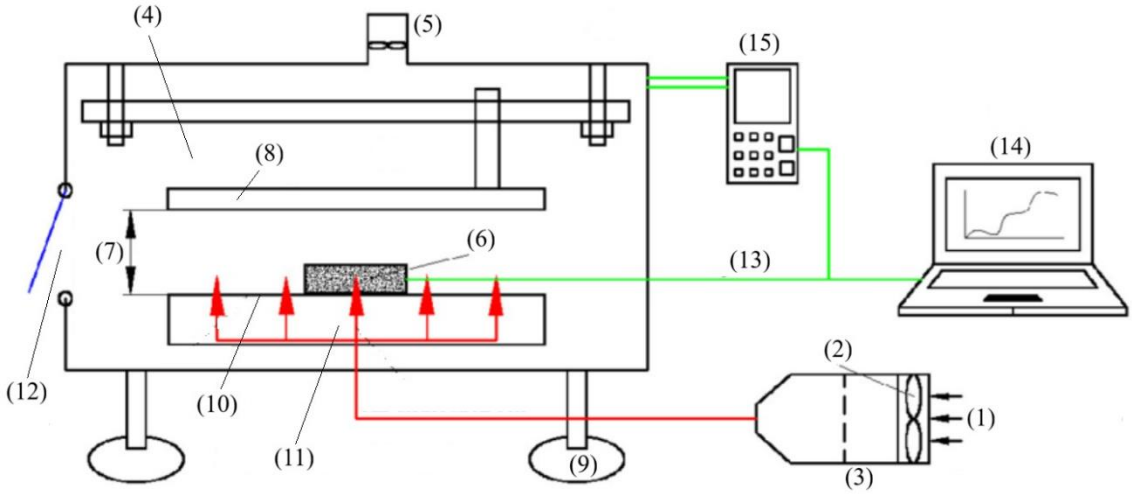

Figure 2. *Schematic diagram of the high-frequency electric field drying system.*

Caption for Figure 2: (1) Inlet air (drying medium); (2) Supply/exhaust fan delivering the drying medium into the drying chamber; (3) Electric resistance heater used to heat the drying medium (inlet air) when the system operates in combination with convective drying; this component is not required if convective assistance is not applied; (4) High-frequency drying chamber (housing the drying material), shielded with a metallic enclosure to prevent electromagnetic leakage; (5) Exhaust fan discharging high-humidity air to the environment; (6) Drying material placement zone, where the material absorbs electromagnetic energy and generates volumetric heat; (7) Distance between the two electrodes; the inter-electrode space forms the electric field region where the drying material is positioned; (8) Upper electrode; (9) Drying chamber support/base; (10) Lower electrode; (11) Air distribution plenum, ensuring uniform distribution of heated air within the drying chamber; (12) External infrared

measurement surface; (13) Fiber-optic temperature sensor, measuring material temperature without interference from the electromagnetic field; (14) Computer-based monitoring system for displaying and storing temperature–time–process data; (15) Controller unit, regulating high-frequency power output and acquiring sensor signals.

Operating principle of the drying system: Ambient air is drawn into the system through the air inlet (1) by means of the fan (2). The airflow subsequently passes through the electric resistance heater (3), where it is heated to the desired temperature before being supplied to the drying chamber.

The heated air is introduced into the drying chamber (4) via the air distribution plenum (11), which ensures uniform airflow distribution throughout the chamber. This airflow serves to remove the moisture evaporated from the material during the drying process.

Inside the drying chamber, the upper electrode (8) and lower electrode (10) are connected to a high-frequency power generator, creating a high-frequency electromagnetic field within the inter-electrode gap (7). The material sample to be dried (6) is positioned between the two electrodes, located in the region of maximum electric field intensity.

During operation, under the influence of the high-frequency electric field, polar water molecules within the material continuously oscillate and rotate in response to the alternating electric field. This polarization–depolarization phenomenon results in dielectric losses, generating heat directly throughout the entire volume of the material. Consequently, the material is heated uniformly from the inside outward, promoting rapid moisture evaporation.

The water vapor generated during drying is carried away by the hot airflow and discharged from the drying chamber through the exhaust system (5), thereby maintaining stable thermal and humidity conditions within the chamber.

The temperature of the material sample throughout the drying process is continuously monitored using a fiber-optic temperature sensor (13), ensuring accurate measurement without interference from the high-frequency electromagnetic field. The sensor signals are transmitted to the controller (15) and subsequently displayed and stored on the monitoring computer (14).

Based on feedback signals regarding temperature and drying status, the controller (15) automatically regulates the high-frequency power supplied to the electrodes, as well as the operating modes of the electric heater (3) and the fan (2), ensuring process stability and achieving the target final moisture content.

Additionally, the external surface temperature of the drying chamber can be monitored using an infrared measurement device (12) installed outside the chamber to ensure operational safety and evaluate heat distribution within the system.

3.2. Results of the calculation, design, and fabrication of the high-frequency electric field drying system

3.2.1. Results of the material balance and energy balance calculations

By applying the calculation procedure from Equation (1) to Equation (12), as presented in Section 2.2, *"Calculation and Design Methodology,"* the material balance and energy balance for the drying process of seasoned anchovy were determined. The calculated results are summarized in Table 1.

Table 1. *Mass and energy parameters required for the design of the drying system.*

No	Parameters	Symbol	Unit	Value
1.	Drying system capacity	G_1	Kg/batch	1000
2.	Drying time per batch	τ_s	h	1.2
3.	Initial moisture content of seasoned anchovy raw material	W_1	%	70
4.	Required final moisture content of the product	W_2	%	8
5.	Mass of product obtained after drying	G_2	Kg/batch	326.1

6.	Amount of water evaporated during the drying process	W	Kg/batch	673.9
7.	Amount of dry matter contained in anchovies	G_{ck}	Kg/batch	300
8.	Amount of water contained in the raw material before drying	W_n	Kg/batch	700
9.	Amount of water remaining in the product after drying	W_{cl}	Kg/batch	26.1
10.	Heat required to raise the temperature of the dry matter of seasoned anchovies from $t'_1 = 25^0C$ to $t'_2 = 65^0C$	Q_1	kJ/batch	15600
11.	Heat required to raise the temperature of the water contained in seasoned anchovies from $t'_1 = 25^0C$ to $t'_2 = 65^0C$	Q_2	kJ/batch	117208
12.	Heat required to evaporate the amount of water W (kg/batch) contained in seasoned anchovies	Q_3	kJ/batch	1583665
13.	Heat required to raise the temperature of the tray containing seasoned anchovies from $t'_1 = 25^0C$ to $t'_2 = 65^0C$	Q_4	kJ/batch	1560
14.	Heat required to raise the temperature of the air in the drying chamber from $t'_1 = 25^0C$ to $t'_2 = 65^0C$	Q_5	kJ/batch	1560
15.	Heat loss through the enclosure structure of the high-frequency drying chamber	Q_6	kW	19.9
16.	Heat supplied to the drying process of seasoned anchovies by high-frequency electric current	Q	kW	417.95

Mass and energy balance calculations have determined the mass of dried product obtained, the amount of water evaporated, and the energy required for the drying process. These parameters are essential for establishing product norms, estimating production costs, and determining the total heat demand of the drying operation. In particular, they provide a fundamental basis for the calculation and design of the high-frequency electric drying system.

3.2.2. Design calculation of the drying system

Using equations (13) to (25) as presented in Section 2.2, "Design Calculation Method," the high-frequency electric drying system was calculated and designed. The results obtained after the calculations have been summarized and are presented in Table 2.

Table 2. *Technical parameters of the drying chamber required for the design of the high-frequency electric drying system.*

No	Parameters	Symbol	Unit	Value
1.	Volume of material occupying space in the drying chamber	V_{ngl}	m^3	1.82
2.	High-frequency electric current frequency	f	Hz	2.7×10^7
3.	Dielectric loss factor of the material	ε''	-	8
4.	Dielectric power absorbed in the seasoned anchovy material	P	W	417.95×10^3
5.	Electric field intensity between the two drying electrodes	E	V/m	4371.74
6.	Distance between the two drying electrodes	d	m	0.1

7.	Applied base voltage across the two drying electrodes	U	kV	0.44
8.	Operating voltage applied across the two drying electrodes	U_{lv}	kV	0.66
9.	Penetration depth of the electromagnetic field into the moist material during drying	d_e	m	0.044
10.	Thickness of the seasoned anchovy drying material layer	d_{vl}	m	0.025
11.	Total tray area for holding seasoned anchovies	A_{sum}	m^2	72.8
12.	Length of the electrode plate, which is also the length of the drying material support rack	D	m	3.2
13.	Width of the electrode plate, which is also the width of the drying material support rack	R	m	2.4
14.	Area of the rack holding drying trays containing the drying material	$A_{chamber}$	m^2	7.68
15.	Number of tray layers containing seasoned anchovies in the drying chamber	N	-	10
16.	Calculate the height of the drying chamber	H	m	1.8
17.	Calculate the volume of the drying chamber	$V_{chamber}$	m^3	13.824
18.	Number of air changes (air exchange rate)	n	Lần/h	12
19.	Calculate the airflow rate of the exhaust–supply fan	L_q	m^3/h	165.9
20.	Electric motor power of the exhaust fan (3-phase motor, 380 V, 50 Hz)	N_{mq}	kW	1.5

The calculated results, summarized and presented in Table 2, provide all necessary data for the design and fabrication of the high-frequency electric field drying system.

AutoCAD 2024 software was used to develop the overall assembly drawings of the drying system, as well as detailed technical drawings for each component and piece of equipment within the system.

The components and equipment were manufactured using appropriate mechanical machining processes. The final stage involved the installation and integration of all components to complete the drying system. This stage requires a high level of technical expertise and professional competence to ensure accuracy and operational safety.

After completion of the mechanical assembly, the next step was the design and installation of the measurement and automatic control system for the drying process, in order to maximize the operational efficiency of the system.

The completed high-frequency electric field drying system is illustrated in Figure 3

The high-frequency electric field drying system is equipped with intelligent automatic measurement and control. This system represents one of the first locally developed radio frequency drying systems for seafood processing in Vietnam, representing a technically complete solution with fully mastered technology. Following this publication, the system is expected to be widely applied in practical production.

Figure 3. *High-frequency electric field drying system with a capacity of 1000 kg per batch.*

3.3. Experimental evaluation of the stable operation of the drying system

Two identical samples of seasoned anchovies were prepared, having the same initial moisture content and mass. One sample was dried using the newly fabricated high-frequency electric field drying system (Figure 3), while the other was dried using a conventional convective drying system. The objective functions of interest were defined as follows: y_1 (%) represents the moisture content of the seasoned anchovies as a function of drying time; y_2 (kWh/kg) represents the specific energy consumption required to produce 1 kg of product; y_3 represents the sensory quality of the product. The sensory quality was evaluated using a 10-point scale, where a score of 10 corresponds to the highest quality and 0 to the lowest quality. The experimental results are presented in Figures 4, 5, and 6.

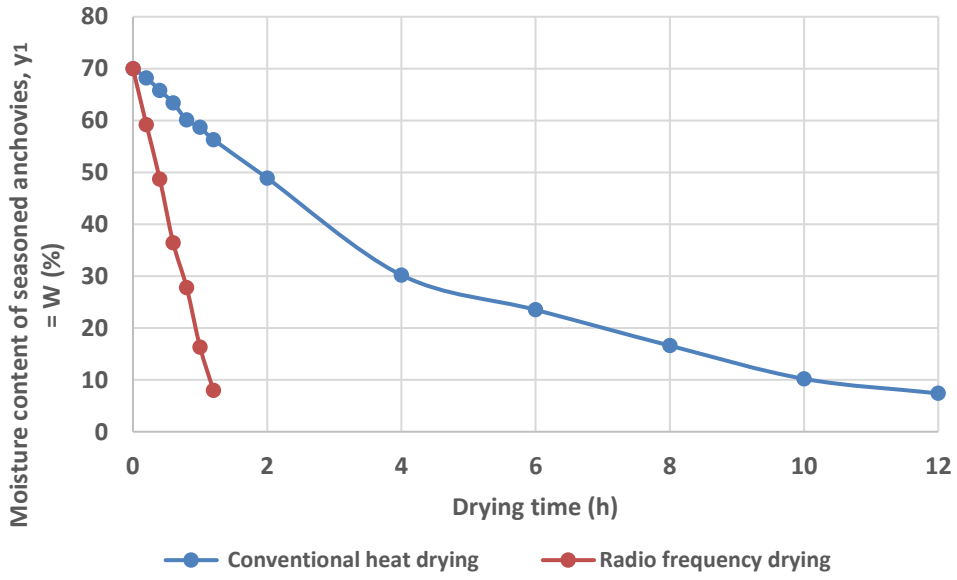

Figure 4. *Relationship between the moisture content of seasoned anchovies and drying time*.

For the convective drying method, the moisture content of the seasoned anchovies decreases relatively slowly and continuously throughout the experimental period, from approximately 70% to below 10% after nearly 12 hours of drying. The moisture reduction curve becomes more gradual and nearly linear in the later stage, indicating that the process is predominantly governed by internal moisture diffusion from the core of the material to its surface.

In contrast, the high-frequency electric field drying method exhibits a significantly faster moisture reduction rate, particularly during the initial stage. The moisture content decreases from about 70% to below 10% within approximately 1–1.5 hours. Volumetric heating generated by the high-frequency electric field enables energy to be directly distributed throughout the material bulk, increasing the internal vapor pressure within the product structure and strongly enhancing moisture migration.

These results demonstrate that high-frequency drying can substantially shorten the drying time compared to conventional convective drying. Consequently, it has the potential to reduce specific energy consumption per unit mass of product and to minimize prolonged thermal exposure that may adversely affect sensory quality. However, for a comprehensive evaluation of the technological performance, additional indicators such as actual energy consumption and post-drying product quality should also be considered.

Figure 5 illustrates the relationship between specific energy consumption (kWh/kg) and product moisture content, revealing a clear difference between the two drying methods. At the same final moisture level, the high-frequency electric field drying method consistently exhibits lower energy consumption than conventional convective drying. Specifically, at a product moisture content of approximately 6%, the energy consumption of the convective method is about 3.5 kWh/kg, whereas that of the high-frequency method is only around 3.1 kWh/kg. A similar trend is maintained throughout the entire investigated moisture range (6–12%), with a relatively stable difference of approximately 0.3–0.4 kWh/kg.

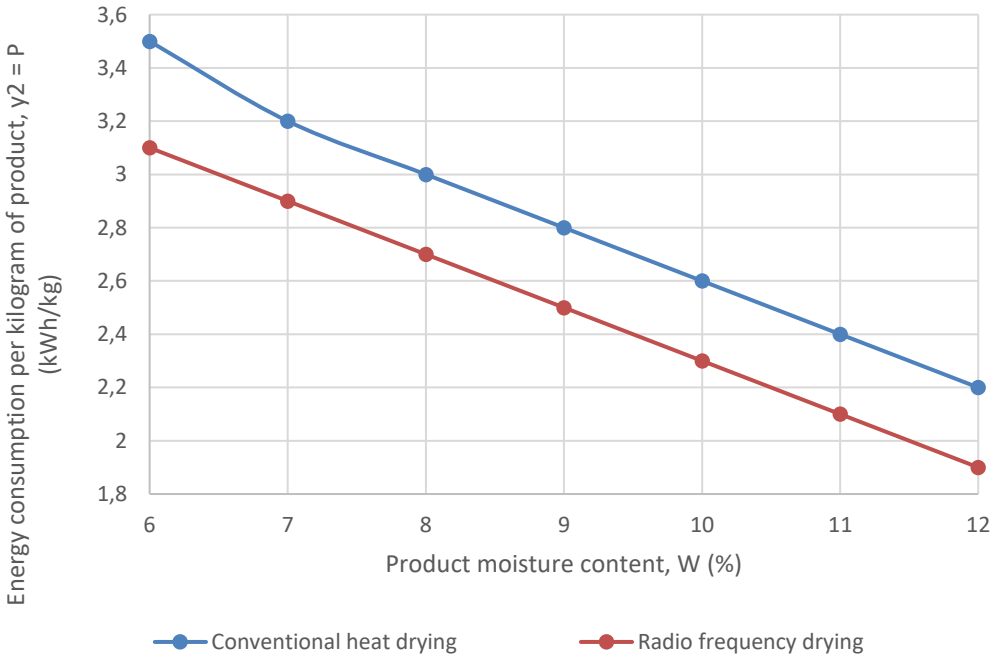

Figure 5. *Relationship between the specific energy consumption for drying 1 kg of seasoned anchovies and the product moisture content.*

Figure 5 also shows that as the product moisture content increases, the specific energy consumption decreases for both drying methods. This reflects the fact that removing strongly bound moisture in the final stage requires more energy than removing free moisture in the initial stage. However, due to the volumetric heating mechanism and reduced heat losses to the surrounding environment, the high-frequency drying method utilizes energy more efficiently, particularly in the low-moisture region—which is typically the most energy-intensive stage of the drying process.

These findings further support the conclusion that high-frequency electric field drying not only shortens the drying time but also has the potential to reduce specific energy consumption per unit mass of product, thereby improving the overall economic efficiency of the process.

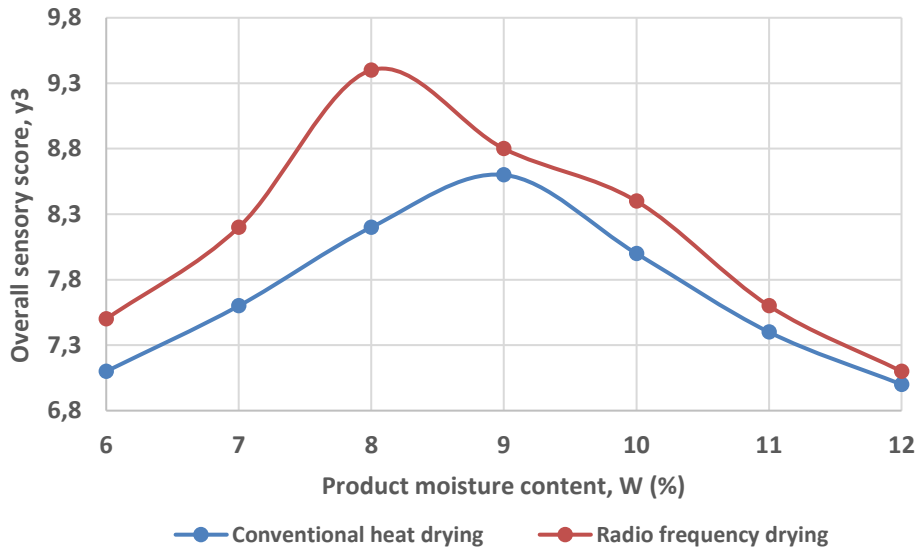

Figure 6. *Relationship between the sensory quality of dried seasoned anchovies and the product moisture content.*

Figure 6 illustrates the relationship between the overall sensory score (y_3) and product moisture content. It can be observed that the sensory quality of seasoned anchovies is strongly influenced by both the final moisture content and the drying method.

For both methods, the sensory score tends to increase as the moisture content decreases from 12% to approximately 8–9%, and then declines when the moisture content is further reduced to 6%. This indicates the existence of an optimal moisture range at which the product achieves a balance among texture, chewiness, color, and characteristic flavor.

Specifically, the high-frequency drying method attains the highest sensory score of approximately 9.4 at a moisture content of about 8%, whereas the convective drying method reaches a lower maximum value of around 8.6–8.7 at a moisture content close to 9%. At all investigated moisture levels, the sensory scores of the high-frequency–dried samples are consistently higher than those of the convectively dried samples. This can be attributed to the shorter thermal processing time and the volumetric heating mechanism of the high-frequency method, which help minimize discoloration, structural shrinkage, and flavor degradation associated with prolonged heating.

When the moisture content decreases to an excessively low level (approximately 6%), the sensory scores for both methods decline markedly, likely because the product becomes overly dry, hard, and less acceptable from a sensory perspective. These findings indicate that selecting an appropriate final moisture content is as important as choosing the drying method itself. Moreover, high-frequency electric field drying demonstrates a clear advantage in terms of sensory quality across the entire investigated range.

Experimental validation demonstrates that seasoned anchovies dried using the high-frequency electric field method exhibit excellent quality, superior to those produced by conventional drying. Moreover, the high-frequency electric field drying system (Figure 3) operated stably throughout the entire drying process. Therefore, the system is fully capable of being applied in practical production.

4. Conclusions

The research results demonstrate that high-frequency electric field drying is markedly more effective than conventional convective drying for processing seasoned anchovies. The high-frequency drying method significantly reduces the drying time, achieving a reduction of approximately 90%, while also decreasing the specific energy consumption per unit mass of product by 10–12%. In addition, the sensory quality of products dried by the high-frequency method is consistently higher (9.4 compared with 8.6) across the entire investigated moisture range. The optimal moisture content is approximately 8–9%, at which the overall sensory score reaches its maximum value.

The high-frequency electric field drying system developed in this study operated stably throughout the experimental process, confirming its technical feasibility and potential for practical industrial application. These findings indicate that high-frequency electric field drying is an effective technological solution, contributing to improved product quality and enhanced economic efficiency in seafood processing.

Acknowledgments

The author thanks Head of Lab B108 “Food Engineering and Technology”, Department of Food Technology, Faculty of Chemical and Food Technology, HCMC University of Technology and Engineering, Vietnam, for their support and help on carrying out the experiments

Conflict of Interest

The authors declare no conflict of interest

REFERENCES

[1] J. Wang and J. Tang, “Radio frequency and microwave alternative treatments for food pasteurization and sterilization,” *Journal of Food Engineering*, vol. 53, no. 3, pp. 257–266, 2001.
[2] A. Chen, F. Wan, and G. Ma, “Radio frequency vacuum drying study on the drying characteristics and quality of *Cistanche* slices and analysis of heating uniformity,” *Foods*, vol. 13, no. 17, p. 2672, 2024, doi: 10.3390/foods13172672.
[3] L. Ren, Z. Zheng, and H. Fu, “Hot air-assisted radio frequency drying of corn kernels: Effects on structure and physicochemical properties of starch,” *International Journal of Biological Macromolecules*, vol. 267, art. no. 131470, 2024.
[4] Li *et al*., “Combined radio frequency heating and pulsed vacuum technology to enhance drying characteristics and heat–mass transfer in peanut pod drying,” *Innovative Food Science & Emerging Technologies*, vol. 102, art. no. 103976, 2025.
[5] M. Zhang, J. Tang, A. S. Mujumdar, and S. Wang, “Trends in microwave-related drying of fruits and vegetables,” *Trends in Food Science & Technology*, vol. 17, no. 10, pp. 524–534, 2006.
[6] S. Jiao, J. A. Johnson, J. Tang, and S. Wang, “Industrial-scale radio frequency treatments: Heating uniformity and energy efficiency,” *Food Engineering Reviews*, vol. 4, pp. 1–16, 2012.
[7] C. T. Tuan, D. T. K. Linh, and N. T. Dung, “Designing and manufacturing a vacuum frying system with intelligent controlling,” *J. Tech. Educ. Sci.*, no. 77, Jun. 2023, doi: 10.54644/jte.77.2023.1374.
[8] L. Giurgiulescu, L. T. Phong, T. K. Linh Do, and N. T. Dzung, “Study on designing and manufacturing the DS-12 freeze-drying system using infrared radiation heating process,” *J. Tech. Educ. Sci.*, vol. 19, no. 3, 2024, doi: 10.54644/jte.2024.1579.
[9] L. Q. Lieu, L. Giurgiulescu, N. V. Suc, N. T. Dzung, “Multi-objective optimization of vacuum frying process conditions for jackfruit using the restricted area method (RAM) with combination criteria R,” *J. Tech. Educ. Sci.*, vol. 20, no. 4, 2025, doi: 10.54644/jte.2025.1996.
[10] N. T. Dzung, T. K. Linh Do, and C. T. Tuan, “Study on designing and manufacturing the freeze drying system with the process of freezing moist materials inside the freeze drying chamber to preserve valuable products,” *J. Tech. Educ. Sci.*, no. 70B, Jun. 2022, doi: 10.54644/jte.70B.2022.1136.
[11] T. K. V. Linh, Q. P. Phu, T. A. P. Dao, and N. T. Dzung, “Building and solving the mathematical model of transient heat transfer during the peanut roasting process to determine the roasting parameters,” *Carpathian Journal of Food Science and Technology*, vol. 14, no. 4, pp. 79–88, 2022, doi: 10.34302/crpjfst/2022.14.4.6.
[12] V. C. Hoang, M. L. Tam, P. P. Quoi, L. Giurgiulescu, and T. N. Dzung, “Mathematical model study to optimize the freeze drying process for production of dried yogurt,” *Carpathian Journal of Food Science and Technology*, vol. 16, no. 4, pp. 151–163, 2024, doi: 10.34302/crpjfst/2024.16.4.12.
[13] D. P. Van, T. P. Hoan, D. T. N. Dung, P. K. Dung, L. Giurgiulescu, and N. T. Dzung, “Development of a mathematical model to determine the moisture diffusivity of an infinite flat slab drying material: Application to freeze-drying of yogurt,” *Carpathian Journal of Food Science and Technology*, vol. 17, no. 3, pp. 41–53, 2025, doi: 10.34302/2025.17.3.4.

Lieu Le Quang
College of Fisheries and Food Technology, Vietnam
Phone: 0915844515
Email: lieucdntsmb2@gmail.com ORCID: https://orcid.org/0009-0000-8722-8873

Liviu Giurgiulescu
Chemistry-Biology Department
Technical University of Cluj Napoca, North Universitary Center of Baia Mare, Romania.
Email:giurgiulescu@gmail.com. ORCID: https://orcid.org/0000-0002-6482-3052

Hung Do Xuan
National College of Education, Ho Chi Minh City.
Email: hungdoxuan@ncehcm.edu.vn; Tel: 0933.789.032

Dzung Nguyen Tan
Department of Food Technology; Faculty of Chemical and Food Technology;
HCM City University of Technology and Engineering, Vietnam;
No 01, Vo Van Ngan Street, Thu Duc Ward, HCM City.
Phone: 0918801670
Email:tandzung072@hcmute.edu.vn. ORCID: https://orcid.org/0000-0002-2482-2098